

Lawrence Berkeley National Laboratory

Recent Work

Title

SOME NEW DEVELOPMENTS IN DIRECT REACTIONS INDUCED BY HEAVY IONS

Permalink

<https://escholarship.org/uc/item/5xx113fj>

Author

Oertzen, W. von

Publication Date

1973-04-01

Presented at the Minerva Symposium
on Physics, Rehovoth, Israel,
April 2-4, 1973

LBL-1678

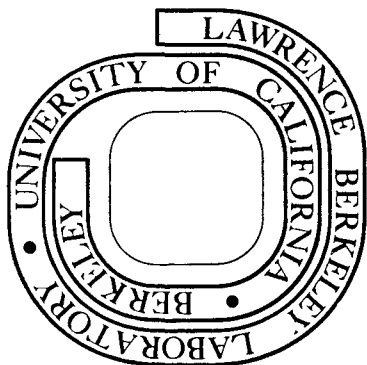
c.1

SOME NEW DEVELOPMENTS IN DIRECT REACTIONS
INDUCED BY HEAVY IONS

W. von Oertzen

April 1973

Prepared for the U. S. Atomic Energy Commission
under Contract W-7405-ENG-48



For Reference

Not to be taken from this room

LBL-1678

c.1

DISCLAIMER

This document was prepared as an account of work sponsored by the United States Government. While this document is believed to contain correct information, neither the United States Government nor any agency thereof, nor the Regents of the University of California, nor any of their employees, makes any warranty, express or implied, or assumes any legal responsibility for the accuracy, completeness, or usefulness of any information, apparatus, product, or process disclosed, or represents that its use would not infringe privately owned rights. Reference herein to any specific commercial product, process, or service by its trade name, trademark, manufacturer, or otherwise, does not necessarily constitute or imply its endorsement, recommendation, or favoring by the United States Government or any agency thereof, or the Regents of the University of California. The views and opinions of authors expressed herein do not necessarily state or reflect those of the United States Government or any agency thereof or the Regents of the University of California.

SOME NEW DEVELOPMENTS IN DIRECT REACTIONS INDUCED BY
HEAVY IONS*

W. von Oertzen

Max Planck Institut für Kernphysik
69 Heidelberg

and

Lawrence Berkeley Laboratory
University of California
Berkeley, California 94720

April 1973

Reactions induced by heavy ions have been extensively studied in recent time (see for example the recent topical conferences). Specifically, direct reactions induced by heavy ions like elastic and inelastic scattering and transfer reactions rely on rather complicated experimental techniques for particle identification and methods of theoretical analysis. There has been in recent time considerable progress in both experimental techniques and in the understanding of the reaction mechanisms. At present stage nuclear structure studies with direct reactions induced by heavy ions should indeed yield the information people believed should be obtainable. The situation is, however, by no means clear in all respects and there is considerable work to be done on the new improved accelerators to establish the heavy ion reactions as the specific spectroscopic tool they are expected to be.

I will at first shortly discuss a few new experimental techniques, then show some rather specific examples of heavy ion reactions which show their unique possibilities, and finally discuss some new concepts which were developed for the understanding of the transfer reactions.

I. PROGRESS IN EXPERIMENTAL TECHNIQUES

The study of heavy ion reactions relies on an adequate identification of the reaction products and on high energy resolution. It seems to be rather obvious by now that the system which will have both, a complete identification of the reaction product, as well as the large solid angle and intrinsic energy resolution to allow measurements with thin targets - is the magnetic spectrometer with a focal plane detector. Such a system is used at the 88-inch cyclotron in Berkeley.¹ In principle, four quantities have to be measured to identify completely a particle and to determine its momentum (energy) spectrum.

These quantities are: Z-nuclear charge, q-charge state of ion while being analyzed in the magnet (at sufficiently high energies $q = Z$ with 100%), m-mass and E-energy or p-momentum. In the system used in Berkeley¹ a resistive-wire proportional counter is placed in the focal plane. The measurement of $\Delta E/\Delta X$, position (or radius ρ) and time-of-flight t , (using a scintillator foil as start detector and a scintillator behind the proportional counter) yields three parameters.

$$\textcircled{1} \left(\frac{\Delta E}{B\rho} \right) \sim M^2 \left(\frac{Z}{q} \right)^2; \quad \textcircled{2} \frac{\Delta E}{t^2} \sim Z^2; \quad \textcircled{3} B\rho \cdot t = \frac{M}{q};$$

$$\text{or } \Delta E \sim \frac{Z^2 M}{E}$$

Three parameters are usually sufficient at high energies and light projectile masses. Figure 2 gives an illustration of the two-dimensional matrix of the parameters $\Delta E/\Delta X$ and t .

With a solid angle of 1-2 msr sufficiently thin targets can be used in experiments to obtain resolutions of 100-150 keV at 100 MeV particle energy.

Figure 1 gives as an illustration single nucleon transfer reactions induced by ^{16}O and ^{12}C on ^{208}Pb . Still using a large solid angle spectra of single nucleon transfer reactions with good resolution are rather expensive (in terms of accelerator time) compared to conventional transfer reactions. Accelerator time can be saved in using measurements of γ -rays.

A recently² applied method which employs coincidences between γ -rays and reaction products gives (with thick targets) an excitation function from the shape of the γ -ray line. The γ -rays are affected by the changing Doppler-shift due to the changing velocity as function of the depth within the target substance. In the same way angular distributions have been obtained from the shape of free γ -ray in ($^{13}\text{C}, ^{12}\text{C}$) neutron transfer reactions. Figure 3 illustrates in an example how a complete angular distribution is obtained from one measurement of γ -rays. In this case the Doppler-shift observed depends on the reaction angle. This method is, of course, only applicable to excited states, however, is extremely efficient in terms of accelerator time. (The angular correlation of the γ -rays - if not isotropic - has to be known.)

Finally the higher energy of the heavy ions from the new accelerators will bring considerable advantages for experimental and theoretical reasons. Target problems which play a considerable role in heavy ion reactions become less restrictive due to smaller energy losses. For many transfer reactions the kinematical restrictions (as discussed later) become smaller and a large abundance of reaction products is observed (Fig. 2).

II. SOME SPECIFIC ASPECTS OF HEAVY ION REACTIONS

A. Nuclear and Coulomb Effects in Elastic and Inelastic Scattering

The elastic and inelastic scattering of heavy ions on target nuclei with large Z, as for example of ^{16}O on ^{58}Ni or ^{208}Pb (at 60 MeV or 104 MeV,

respectively) exhibit features which are determined by a strong Coulomb interaction competing with the nuclear forces. The signs of the two forces are opposite and this fact leads to peculiar properties of the elastic and inelastic cross sections. Figure 4 illustrates³ the shape of angular distributions in elastic scattering; the real potential induces fine structure in the grazing region, where the differential cross section deviates from Rutherford scattering. Even more drastically the effects are seen in inelastic scattering which depends on the derivative of the nuclear and Coulomb potentials. The nuclear effect is now strongly localized (the derivative of a Woods-Saxon potential is peaked at the nuclear surface) and a cancellation occurs at a given radius due to the opposite signs of the two terms. A pronounced dip is thus observed in the angular distributions at the angle where the scattering orbit goes through a distance in the interaction region where the cancellation occurs (Fig. 5). Both effects are extremely sensitive to details of the total potential, i.e., to both the real and imaginary part.⁴

B. Elastic Transfer

Interference effects in themselves are usually very sensitive to details of the reaction process. The second example also involves interferences between two competing processes. In elastic transfer, a transfer reaction of the type $A(B,A)B$ with $B = (A + c)$, interferes coherently with the elastic scattering $A(B,B)A$. In the center of mass system the scattering angles are connected by the relation $\theta_B = \pi - \theta_A$. The two reactions are indistinguishable and their interference gives rise to structures in the angular distributions which are similar to those observed in Mott-scattering.^{5,6} Using the semiclassical description of the transfer process (see also section III)

$\sigma_{tr}(\pi - \theta) = P_{tr} \sigma_{el}(\pi - \theta)$, with P_{tr} transfer probability, we obtain for the total differential cross section

$$\sigma_{total}(\theta) = \left| \sqrt{\sigma_{el}(\theta)} + (-)^{A+l} \sqrt{P_{tr} \sigma_{el}(\pi - \theta)} \right|^2 .$$

The sign $(-)^{A+l}$ takes into account the proper anti-symmetrization of the cores (A - number of fermions in the core) and the symmetry property of the bound state of the transferred particle c (l - angular momentum in the bound state). For $P_{tr} \equiv 1$ and independent of angle the expression for Mott-scattering is obtained. The interference structure depends on the Sommerfeld parameter $\eta = Z_1 Z_2 e^2 / \hbar v$ just like in real Mott-scattering and, of course, on the ratio of the two amplitudes interfering (in Mott-scattering the forward and backward scattering amplitudes are equal yielding symmetry by 90° cm). In systems where elastic transfer can occur the region of interference is at those angles where it has comparable amplitude with the elastic scattering. Figure 6 shows as an illustration the scattering of ^{19}F on ^{18}O and ^{16}O . In these systems transfer of a proton and triton can occur. Two aspects of this example are worthwhile to mention. 1) The extraction of the spectroscopic information - the spectroscopic factors for the decomposition of ^{19}F into triton or proton plus ^{16}O or ^{18}O core, does not depend, as usually, on an absolute cross section but on the shape of an interference pattern. 2) In the present experiment⁶ the ground state of ^{19}F was not resolved from closely lying states of 150 keV excitation. However, as can be seen from Fig. 6, the small transfer cross section is amplified due to the coherence with elastic scattering. The unresolved states adding incoherently (typical strength is shown by dotted line in Fig. 6) just fill slightly the minima in the angular distribution and do not affect the information in the data.

These aspects in this type of experiment could be rather important for heavier ions, because the energy resolution often will not be sufficient to separate the final states if projectiles with masses greater than 40 are involved.

C. Multi-Nucleon Transfer

A third important aspect of heavy ion induced direct reactions is the possibility to transfer many nucleons or large amounts of nuclear matter. Quite a few experiments have been reported where exotic (neutron rich) nuclei are produced in a high energy induced transfer reaction.⁷ The transfer of many nucleons possibly has to be considered as a many step process. In a semiclassical description the reaction will consist of a product of many single probabilities (transfer of x individual nucleons)

$$\sigma_{tr} = P_1 \cdot P_2 \cdot P_3 \dots P_x \cdot EF \sigma_{el} .$$

with $P_i \approx 10^{-1} - 10^{-2}$.

The cross sections for multi-nucleon transfer reactions therefore are expected to be rather small, unless certain correlation effects occur (see also section IIIa) and lead to an enhancement expressed in terms of enhancement factors EF. Different correlated groups could be transferred one after the other and particular effects of two-step process will show up in these cases.

Typical two-step processes could be involved in reactions like $(^{16}_0, ^{13}_C)$ which could be viewed as a transfer of two protons and a consecutive transfer of a neutron. Generally, the transfer of many nucleons will consist of a coherent sum of many processes in which different substructures in the transferred nucleons can contribute (for example $(^{16}_0, ^{14}_C - ^{13}_C)$ or $(^{16}_0, ^{14}_N - ^{13}_C)$ as possible sequences for the $(^{16}_0, ^{13}_C)$ reaction).

Recent calculations⁸ for example have shown that the interference between inelastic scattering before transfer and transfer before inelastic scattering processes can lead to a flattening of the shape of angular distributions (Fig. 7) (if the interference is destructive). In this coupled channel calculation the inelastic scattering is considered to have a very large probability, the transfer process is, however, only treated in first order (CCBA).

The transfer of large amounts of nucleons has also to be viewed in terms of macroscopic properties of nuclei as discussed by Swiatecki.⁹ Important parameters in this respect are the liquid drop parameter Z^2/A , and asymmetry. Figure 8 shows as an example the potential energy as function of asymmetry. For two colliding masses, m_1, m_2 , there seems to be a critical asymmetry m_1/m_2 (depending on Z^2/A) below which the lighter mass nucleus is eaten up by the larger target nucleus - forming a heavier compound or residual nucleus - or for larger values of m_1/m_2 the two nuclei redistribute their masses in such a way as to achieve a symmetric two-body configuration. These aspects will be important for the formation of compound nuclei and the transfer of large amounts of nucleons.

III. PROGRESS IN CONCEPTS FOR THE INTERPRETATION OF TRANSFER REACTIONS

A. Semiclassical Models and Window Effects

It has been realized more than 20 years ago by Breit and co-workers¹⁰ that heavy ion reactions can be described by semiclassical models provided the Sommerfeld parameter η , $\eta = Z_1 Z_2 e^2 / \hbar v$ is large relative to unity. If $\eta \gg 1$, the minimum distance in the relative motion becomes large compared to the Broglie wavelength λ , using relation

$$R = \frac{\eta}{k} \left(1 + \frac{1}{\sin \theta/2} \right) = \eta \lambda \left(1 + \frac{1}{\sin \theta/2} \right) \quad (1)$$

Where θ is the scattering angle and R is the minimum distance in the classical orbit determined by the Coulomb field. The semiclassical models assume that the orbits can be described by classical equations and the transfer process by quantal methods, i.e., it has only small influence on the scattering path. It has been realized only recently that the classical orbit description leads to severe restrictions of changes of the important quantities, k , η , θ , if a sizable cross section has to result. It has been found¹⁴ that sub-Coulomb transfer reactions have only large cross sections if the minimum distances R_{\min}^i and R_{\min}^f are equal. Thus, we obtain, $R_{\min}^i = R_{\min}^f$, as a condition which relates changes in η and k in a reaction. An optimum Q -value is obtained (assuming $\theta_i = \theta_f$)

$$Q_{\text{opt1}} = \frac{Z_3 Z_4 - Z_1 Z_2}{Z_1 Z_2} E_{\text{CM}}^i \quad (2)$$

which depends on the amount of charge being transferred in the reaction. This relation still holds approximately at energies above the Coulomb barrier. Modifications are mainly introduced due to possible large (or small) amounts of angular momentum transfer and due to absorption processes. Thus, transfer of charge between a light projectile and a heavy nucleus (1p, 2p α -transfer) is always observed with negative Q -values. All other reactions with non-optimum Q -values (like pick-up of charge from a heavy nucleus) are strongly depressed. Actually the cross section can be shown to depend on a few simple factors which can be discussed independently in a semiclassical model.¹¹ For a given

scattering orbit we have

$$\frac{d\sigma}{d\Omega}(\theta) = \sqrt{\sigma_i/\sigma_{Ri} \cdot \sigma_f/\sigma_{Rf}} \bar{\sigma}(\theta) \cdot P_t(\theta) \cdot F(\Delta D) \quad (3)$$

The cross section depends on a scattering probability. This scattering probability is appropriately described by an average Rutherford cross section $\bar{\sigma}(\theta)$ multiplied with the rates of absorption in the incident and final channel $\sqrt{\sigma_i/\sigma_R \cdot \sigma_f/\sigma_R}$. The factor $F(\Delta D)$ gives the Q-value dependence as function of $\Delta D = |R_{\min}^i - R_{\min}^f|$ which is a measure of the overlap of the ingoing and outgoing scattering states. $P_t(R)$ is the transfer probability which is mainly the form factor squared.

The three factors can be easily calculated numerically using the semiclassical model. It has been shown¹² that the elastic cross section can be rather well described by an exponential function of R_{\min} (see Fig. 9).

$$\frac{\sigma}{\sigma_R} = \begin{cases} 1 ; & , R > R_0 ; \\ 1 - e^{-(R-R_0)/\Delta} & , R \leq R_0 ; \Delta \approx 0.5 \text{ fm} \end{cases} \quad (4)$$

Similarly, it has been shown that $F(\Delta D)$ has a gaussian shape for large angles.

$$F(\Delta D) \sim e^{-\Delta D/\alpha R \lambda^2} \quad (5)$$

With α - the bound state decay constant determined by the binding energy E_B and reduced mass M_C of the transferred particle, $\alpha = (2M_C E_B \hbar^{-2})^{1/2}$. The transfer probability is typically also an exponential as function of the minimum distance.

$$P_t(R) \sim e^{-2\alpha R/(\alpha R)^2} \quad (6)$$

These simple formula can help in many cases to study the chances of a certain experiment. The strong Q-value dependence of the cross section which is virtually contained in all three factors can give extremely small cross sections in the regions of interest. Typical shapes of these windows are shown¹³ in Fig. 10 (experimental) and Fig. 11 (theoretical). Depending on the angle of observation, different factors in expression (3) determine the shape of the Q-value window.

Any reaction product which is emitted from the surface of the nucleus (as a result of a direct or compound reaction) will have to follow a certain trajectory which is determined by the parameters: Charge product Z_3Z_4 , radius R_0 where the particles originate (also absorption radius), and angle of observation θ . If the particles start with tangential velocity, their energy in the final channel has to be determined by Eq. (1). The optimum Q-value in this case would be

$$Q_{opt2} = E^f - E_{cm}^i = Z_3Z_4/2R_0 \left(1 + \frac{1}{\sin^2 \theta/2} \right) - E_{cm}^i \quad (7)$$

The final energy consists typically of a potential energy part, which is the Coulomb potential at R_0 , and a kinetic energy which is determined by the centrifugal barrier (and θ). For an angle θ larger θ_0 the reaction yield as function of E^f or Q scans the absorption probability and the transfer probability as function of minimum distance in a similar way as does the variation of the scattering angle. In Fig. 12 a schematic representation is given which illustrates the close relationship between the occurrence of a

Q-value window and an angle window (for $\theta > \theta_0$). Both values θ_0 and $Q_0 = Q_{opt}$ can thus be related to an absorptive radius R_0 . At angles $\theta < \theta_0$, where the nuclei never touch the matching of orbits of the initial and final channel as discussed for sub-Coulomb transfer reactions¹⁴ becomes the most important factor in determining the reaction yield (Q_{opt1}).

In a purely semiclassical framework the angular momentum transfer is fixed by the change of the parameters η , k , θ . However, in a reaction in which a determined amount of angular momentum is transferred during the quantum mechanical transfer process between definite states, the following prescription may be used to determine the final reaction yield. The grazing angular momentum in the initial channel is determined by;

$$L_{O_i} = k_i R_0 \left(1 + \frac{2\eta_i}{k_i R_0} \right), \quad (8)$$

θ_i is given by Eq. (2).

This angular momentum will give the largest contribution to the reaction; determine L_f by $\vec{L}_i - \vec{\ell} = \vec{L}_f$; then calculate θ_f using for example relation $L_f = \eta_f \text{ctg } \theta_f/2$ for pure Coulomb fields. Having calculated θ_f the ratios $\sigma/\sigma_R(\theta)$ and the average minimum distance and $F(\Delta D)$ can be calculated. In cases of large mismatch, for example transfer of two units of charge, we usually have $\eta_i \gg \eta_f$, $\ell = 0$ and $L_i \gg L_f$ and we obtain $\theta_f \ll \theta_i$. This actually implies that the absorption in the final channel will be smaller compared to that in the initial channel. The cross section will be small unless the grazing angle is much smaller than usually calculated (using R_0 and Eq. (2)). The effects of this decrease in η in the final channel can already be seen in ($^{12}\text{C}, ^{11}\text{B}$) reaction on

^{208}Pb shown in Fig. 13 (Ref. 15). The grazing angle θ_0 stays constant as function of Q value. This is in contrast to DWBA calculations (and simple semiclassical considerations) with optical model parameters which allow sufficient averaging over the initial and final channel. The data actually indicate that the absorption in the incident channel dominates the process as discussed above. Similar conclusions were drawn from work done at Oak Ridge;¹⁶ they actually found, that in the transfer of neutrons $^{208}\text{Pb}(^{12}\text{C}, ^{13}\text{C})^{207}\text{Pb}$ an average orbit including the final channel is followed — leading to a shift of θ_0 as function of the Q-value.

Corresponding to Eq. (3) and Fig. 12 there is always one side of the window which is determined by absorption with $R_{\min} < R_0$, which implies $\theta > \theta_0$ or $E_f > E_0$; and another side which is determined by the overlap of the scattering waves (or classical orbits) with $R_{\min} > R_0$, implying $\theta < \theta_0$ or $E_f < E_0$.

Generally, it can be concluded that the discussion of window effects as function of E_f and θ_f have to be made with clear reference to the value of the fixed variable (θ_f for Q-value window, E_f — for angular window), i.e., on which side of the window the relevant variable is kept fixed.

An illustration of the calculation of the Q-value dependence can be given by ($^{16}\text{O}, ^{14}\text{C}$) reactions on ^{140}Ce , ^{142}Nd , and ^{144}Sm . The ground state Q-values change and the strength going to the ground states changes. In order to compare reactions with the same conditions the factors for absorption, and $F(\Delta D)$ have to be calculated. The result is $P_t(R)$ or $P_t(d_0)$ (with $R = d_0(A_1^{1/3} + A_2^{1/3})$) which can be compared for different target nuclei as the quantity which does not contain kinematical effects or nuclear size effects. Figure 14 shows the transfer probabilities $P_t(d_0)$ for the ($^{16}\text{O}, ^{14}\text{C}$) ground

state transitions for different target nuclei. It is seen that the $N = 82$ nuclei Ce, Nd, Sm show an enhancement by factor 20-30 which is similar to that observed in (t,p) reactions on Sn-isotopes (neutron shells in ^{108}Sn - ^{112}Sn correspond to proton shells in ^{140}Ce , ^{142}Nd , and ^{144}Sm).

B. Finite Range Effects

Important changes in the reaction process compared to the previous discussion are due to the finite mass of the transferred nucleons, also called recoil effects. They are connected to the coordinates of relative motion \vec{r}_i, \vec{r}_f (reaction $A + (b + c) \rightarrow (A + c) + b$ or $A(a,b)B$).

$$\vec{r}_i = \vec{r} + (m_c/M_a) \vec{r}_1 \approx \vec{r}$$

$$\vec{r}_f = \frac{M_A}{M_B} \vec{r} + (m_c/M_B) \vec{r}_1 \approx \frac{M_A}{M_B} \vec{r}$$

which can be approximated by the distance between the two cores \vec{r} . This approximation has been used extensively, because it allows a simple calculation of the transition amplitude. At energies near the Coulomb barrier when the wavelength of relative motion is large compared to $\left(\frac{m_c}{M_a}\right) |r_1|$ the neglect of these terms proportional to r_1 (or r_2) introduces only small errors because the change in phase for the scattering waves is small. At higher energies, however, a complete treatment of all coordinates is necessary. There are two main effects which come into play at higher energies.^{17,18} A change in the contributing angular momentum transfers and loss of the semi-classical conditions. At lower energies and large Sommerfeld parameter η it was observed that the maximum angular momentum transfer ℓ is favored by approximately a factor of 10 over the smaller

values. This fact can be understood semiclassically by taking as a condition for a large cross section that the velocity of the transferred nucleon is constant during the transfer process $\frac{\lambda_1}{R_1} + \frac{\lambda_2}{R_2} = 0$; λ - projections of the internal angular momenta in the initial (ℓ_1) and final channel (ℓ_2) on an axis perpendicular to the reaction plane. Figure 15 gives a simplified illustration of the situation. The preference of the maximum ℓ transfer leads to j -dependence in single nucleon transfer.¹⁹ Thus, for ($^{16}_0, ^{15}_N$) reactions the proton starting with $j_< = \ell - 1/2$ preferentially populates $\ell + 1/2 = j_>$ states whereas ($^{12}_C, ^{11}_B$) reactions preferentially populate $j_<$ states because the proton starts from a $p_{3/2}$ orbit (see Fig. 1). Figure 16 gives an illustration of this j -dependence in single proton transfer reactions on ^{208}Pb for two energies. As the relative velocity increases the transferred particle carries an appreciable amount of the relative momentum (MeV/nucleon) and the picture is changed, the particle will be transferred preferentially in a different way as suggested in lower part of Fig. 12. The j -dependence is thus mainly removed at higher energies (Fig. 17). For the extraction of spectroscopic factors it becomes extremely important to calculate the recoil terms properly.^{15,18}

More precisely, the complete finite range description differs from the previously applied no-recoil approximations^{17,18} in allowing the full space for the coupling of the intrinsic angular momenta in the initial and final channel $\vec{\ell} = \vec{j}_1 - j_2$; $\vec{\ell} = \vec{\ell}_1 + \vec{\ell}_2$. Neglecting recoil terms, i.e., vectors proportional to $\frac{m_c}{M_b} \vec{r}_1$, reduces the non-local transfer operator to a local one, because the additional dependence on vector \vec{r}_1 is removed. The most conspicuous difference between the two operators is, that if the particle m_c is fixed on the interconnection line between the two centers the local transfer operator

has a "parity conserving" symmetry which yields the rule $l_i + l_f + l = \text{even}$. This parity rule applies fairly well at energies below or at the Coulomb barrier, where the transferred particle has to be on the interconnection line during the transfer process.

C. High Energy Reactions

The difference between full finite range calculations and no-recoil-approximations becomes important at higher incident energies and is rather drastic as illustrated in Fig. 16 by the reaction $^{12}\text{C}(^{14}\text{N}, ^{13}\text{C})^{13}\text{N}$ (Ref. 18). The diffraction pattern which is observed in some cases in transfer reactions between light nuclei, where only one parity in the angular momentum transfer contributes, is damped due to the contributions of equal amounts of $l = 1$ and $l = 0$ in the present case. At very high energies above the barrier, i.e., large values of k_i , or large values of energy per nucleon the angular momentum per nucleon L_{o_i}/M_a (this number depends on the size of the nuclei involved) becomes very large. It can be shown that in these cases final states are mainly populated with $l_f \approx L_{o_i}/M_a$. At small scattering angles the main source of angular momentum transfer comes from the redistribution of the masses. This selectivity in the population of final states is rather pronounced and was observed in one, two and three nucleon transfer reactions on light nuclei.²⁰ An example is shown in Fig. 18 for the three nucleon transfer $^{12}\text{C} + ^{12}\text{C} \rightarrow ^9\text{Be} + ^{15}\text{O}$ at three different energies. At higher energies states involving large angular momentum transfer show up stronger and these states then have to be the aligned configurations of three individual nucleons with high spins. (The individual angular momenta are parallel $l_1 + l_2 + l_3 = l_f$; and $l_1 \approx l_2 \approx l_3 \approx L_{o_i}/M_a$.)

Other important features of high energy induced heavy ion reactions are connected with the window effects discussed previously. Clearly the semiclassical matching conditions involving Coulomb orbits and large η will change eventually to the angular momentum matching conditions involving plane waves and small η . The plane wave matching condition involves the condition $L_i \approx L_f$ for the relative angular momenta, if the angular momentum transfer ℓ is small, or also $k_i \approx k_f$. The wave number being $k = \sqrt{2E \mu} / \hbar$, a decrease of the reduced mass corresponding to stripping reactions (increase - pickup) needs a positive Q-value (or negative for pick up). This is in contrast to the situation with charged particle transfer with large values of η where the optimum Q-value is negative. A broadening of the Q-value window can be expected at energies high above the Coulomb barrier (see Fig. 19 as illustration). Spectra of $(^{16}_0, ^{15}_N)$, $(^{16}_0, ^{18}_0)$ reactions²¹ taken at 140 MeV $^{16}_0$ on $^{208}_{Pb}$ or $^{144}_{Sm}$ show a continuous background (Fig. 17) at higher excitation whose origin is unexplained. There are indications that this background is particularly strong at small angles.²²

This phenomenon could be connected with the fact that angular momenta in grazing collisions become rather large at energies well above the Coulomb barrier. Liquid drop calculations²³ indicate that the maximum angular momentum at which a nucleus becomes unstable to fission is approximately $80 \hbar$ at mass 200. Figure 20 illustrates the calculations for different values of the fission barrier. For reactions where the surface angular momentum becomes comparable or larger than the critical value of ℓ_{II} (Fig. 20) complicated processes which involve many degrees of freedom of many nucleons can occur. Single nucleon or two nucleon transfer reactions in these cases should show features which are not anymore compatible with inert core models usually applied. Qualitatively

new phenomena could be expected in collisions and transfer processes, because the limiting angular momenta correspond to internuclear distances where nuclei overlap strongly.

IV. ACKNOWLEDGMENTS

The author is very much indebted to his colleagues at Berkeley for discussions and the access to unpublished data. He thanks in particular B. G. Harvey for the kind hospitality at the 88-inch cyclotron and LBL.

FOOTNOTES AND REFERENCES

* Work performed under the auspices of the U. S. Atomic Energy Commission.

1. B. G. Harvey et al., Nucl. Instr. Methods 104, 21 (1972).
2. K. Haberkant, Thesis MPJ Heidelberg, 1973 and K. Haberkant, E. Grosse et al., to be published.
3. R. A. Broglia, S. Landowne, and A. Winther, Phys. Letters 40B, 293 (1972).
4. F. Videback et al., Phys. Rev. Letters 28, 1072 (1972) and F. Becchetti, in Symposium on Heavy Ion Transfer Reactions, Argonne, 1973 (in press) and references therein.
5. W. von Oertzen, Nucl. Phys. A148, 529 (1970); H. G. Bohlen and W. von Oertzen, Phys. Letters 37B, 451 (1971).
6. A. Gamp et al., Z. f. Physik (in press).
7. A. G. Artulch et al., Nucl. Phys. A168, 321 (1971) and references therein.
8. N. Glendenning, Symposium on Heavy Ion Transfer Reactions, Argonne, 1973 (in press).
9. W. J. Swiatecki, European Conference on Nuclear Physics, Aix-en-Provence (1972), J. de Physique C5-45 (1972).
10. G. Breit et al., Phys. Rev. 87, 74 (1952).
11. R. A. Broglia and A. Winther, Phys. Rep. 4c, 155 (1972).
12. P. R. Christensen, V. I. Manko, F. D. Becchetti, and N. J. Nickles, NBI preprint, Nucl. Phys. (in press).
13. W. von Oertzen, H. G. Bohlen, and B. Gebauer, Nucl. Phys. (in press).
14. P. J. A. Buttle and L. J. B. Goldfarb, Nucl. Phys. A115, 461 (1968).
15. D. Kovar et al., Phys. Rev. Letters (in press) and to be published.
16. J. S. Larson, J. L. C. Ford, R. M. Gaedke et al., Phys. Letters 42B, 205 (1972).

17. D. Brink, Phys. Letters 40B, 37 (1972); also W. von Oertzen, Single and Multinucleon Transfer Reactions in Nucl. Spectroscopy, ed., J. Cerny, Academic Press (in press).
18. R. M. de Vries and K. I. Kubo, Phys. Rev. Letters 30, 325 (1973) and R. de Vries, to be published.
19. D. Kovar et al., Phys. Rev. Letters 29, 1023 (1972).
20. D. K. Scott et al., Phys. Rev. Letters 28, 1659 (1972) and N. Anyas-Weiss et al., Oxford University, Nuclear Physics Laboratory, preprint 49/72.
21. D. Kovar in Symposium on Heavy Ion Transfer Reactions, Argonne, 1973, ANL (in press).
22. J. Galin et al., Nucl. Phys. A159, 461 (1970).
23. S. Cohen, F. Plasil, and W. J. Swiatecki, LBL-1502, preprint.

FIGURE CAPTIONS

- Fig. 1. Spectra of single nucleon transfer induced by ^{16}O and ^{12}C obtained using a magnetic spectrometer (Ref. 19).
- Fig. 2. Two-dimensional matrix of parameters $\Delta E/\Delta X$ and TOF for reactions products from bombardment of ^{208}Pb with 104 MeV ^{16}O . a: $^{16}\text{O}(7^+)$, b: $^{17}\text{O}(7^+)$, c: $^{18}\text{O}(7^+)$.
- Fig. 3. Angular distribution of the reaction $^{90}\text{Zr}(^{13}\text{C}, ^{12}\text{C})^{91}\text{Zr}^*$ (1.205 MeV) at 35 MeV incident energy derived from the shape of the free γ -rays (shown as insert in the figure. The crosses on the full curve illustrate typical errors (Ref. 2)).
- Fig. 4. Deflection function (impact parameter ρ as function of scattering angle θ) and angular distributions of elastic scattering for different strength of nuclear potential (Ref. 3).
- Fig. 5. Angular distributions for elastic and inelastic scattering for ^{16}O on ^{208}Pb . The minimum in the inelastic scattering to the 3^- state occurs at the angle where σ/σ_R starts to deviate from unity. As shown in Fig. 4 at this angle the real potential becomes the same as the Coulomb potential (Ref. 4).
- Fig. 6. Elastic scattering of ^{19}F on ^{18}O and ^{16}O at energies of Ca 5 MeV above the Coulomb barrier. The full curve represents calculations including the transfer of a proton ($2s_{1/2}$) and a triton ($4s$), respectively (Ref. 6). The dotted curve corresponds to non-interfering cross sections.
- Fig. 7. Calculations using a coupled channels Born approximation for 2n-transfer involving inelastic processes in the initial and final channel (Ref. 8).
- Fig. 8. Stationary potential energy of two nuclei as function of the asymmetry (ratio of their masses) for different values of the parameter Z^2/A (Ref. 9).

Fig. 9. Ratios of elastic scattering cross sections to Rutherford scattering at different energies and target nuclei transformed to a common scale,

$$R_{\min} = d (A_1^{1/3} + A_2^{1/3}) \text{ (Ref. 12).}$$

Fig. 10. Spectra of ^{14}C and ^{12}C nuclei from ^{16}O induced reactions on ^{140}Ce illustrating the window effect in the spectra (Ref. 13).

Fig. 11. Calculations (using DWBA) of Q-value windows for the ($^{16}\text{O}, ^{14}\text{C}$) reaction on ^{140}Ce at various incident energies and for different angular momentum transfer (Ref. 13).

Fig. 12. Schematic presentation of variations of R_{\min} with θ_f (E_f fixed) or with E_f (for fixed θ_f) and the corresponding yield curves.

Fig. 13. Angular distributions of proton transfer ($^{12}\text{C}, ^{11}\text{B}$) on ^{208}Pb leading to different final states in ^{209}Bi . The full curves are DWBA calculations (dotted curves are shifted to fit the data) (Ref. 15).

Fig. 14. Transfer probabilities $P_{\text{tr}}(d_o)$ for ($^{16}\text{O}, ^{14}\text{C}$) reactions on various target nuclei deduced using semiclassical models. The reactions on Ce, Nd and Sm are enhanced by a factor of ca 20-30 (Ref. 13).

Fig. 15. Schematic illustration of particle transfer in a semiclassical scattering orbit for small relative velocities (top of figure) and large relative velocities (lower part of figure).

Fig. 16. Angular distributions of the reaction $^{12}\text{C}(^{14}\text{N}, ^{13}\text{C})^{13}\text{N}$ at 78 MeV and DWBA calculations illustrating the damping of the diffraction structure due to contributions of angular momenta with different parity ($\ell = 0$ and $\ell = 1$) (Ref. 18).

Fig. 17. Spectra of proton transfer ($^{16}\text{O}, ^{15}\text{N}$) on ^{208}Pb at 104 MeV and 140 MeV (Ref. 15).

Fig. 18. Selectivity in the three nucleon transfer reaction

$^{12}\text{C} + ^{12}\text{C} \rightarrow ^9\text{Be} + ^{15}\text{N}$ due to varying amounts of the angular momentum per nucleon at various incident energy (Ref. 20).

Fig. 19. Yield of a transfer of charge from light to heavy nucleus (stripping reaction) as function of Q-value and incident energy at the angle of maximum cross section (grazing angle). At high energies the Coulomb dominated Q-value window has to change to corresponding plane wave conditions.

Fig. 20. Limiting angular momenta for nuclei obtained from liquid drop calculations. ℓ_I - designates the angular momentum at which the fission barrier vanishes for a axially symmetric nucleus (Ref. 23).

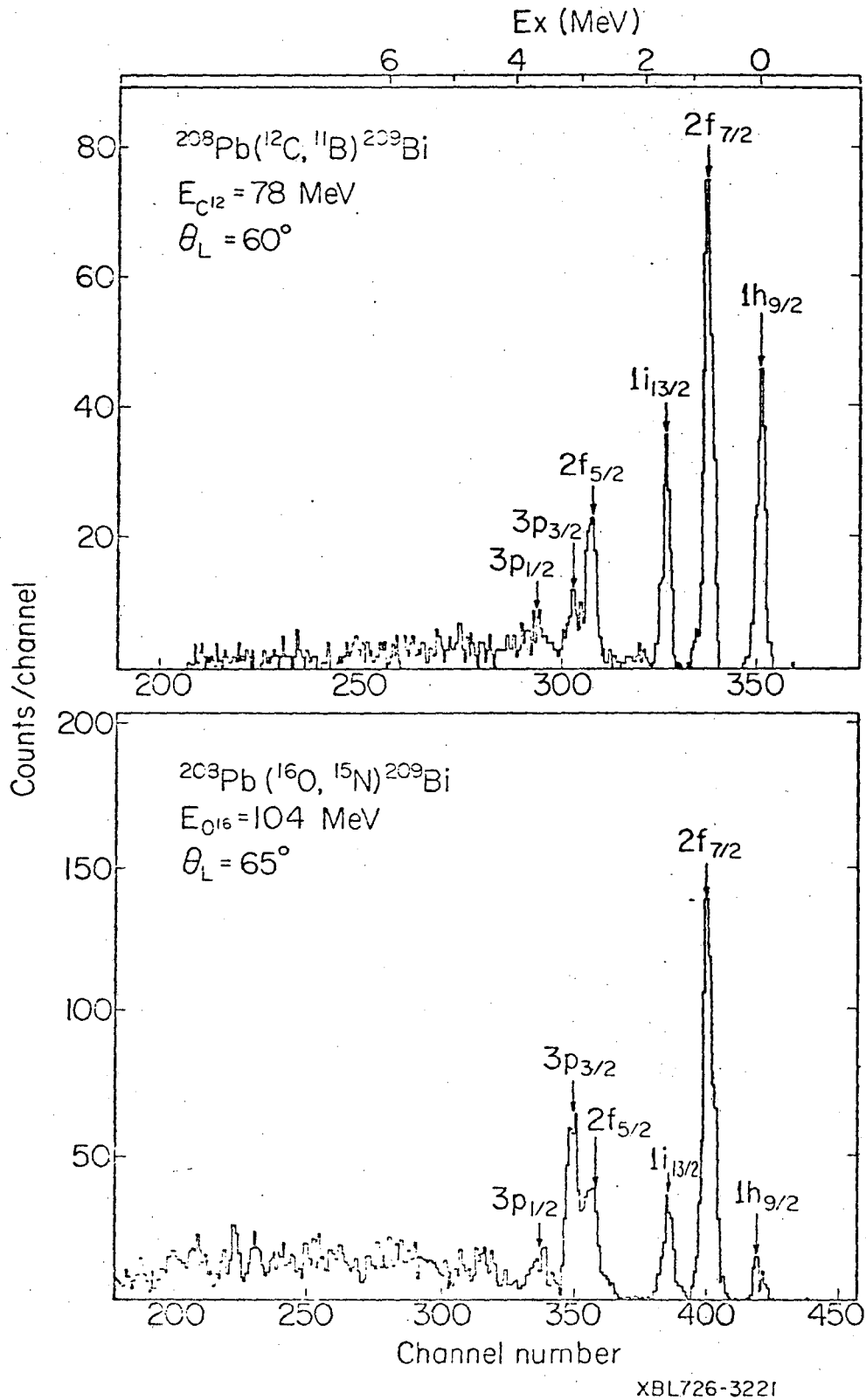
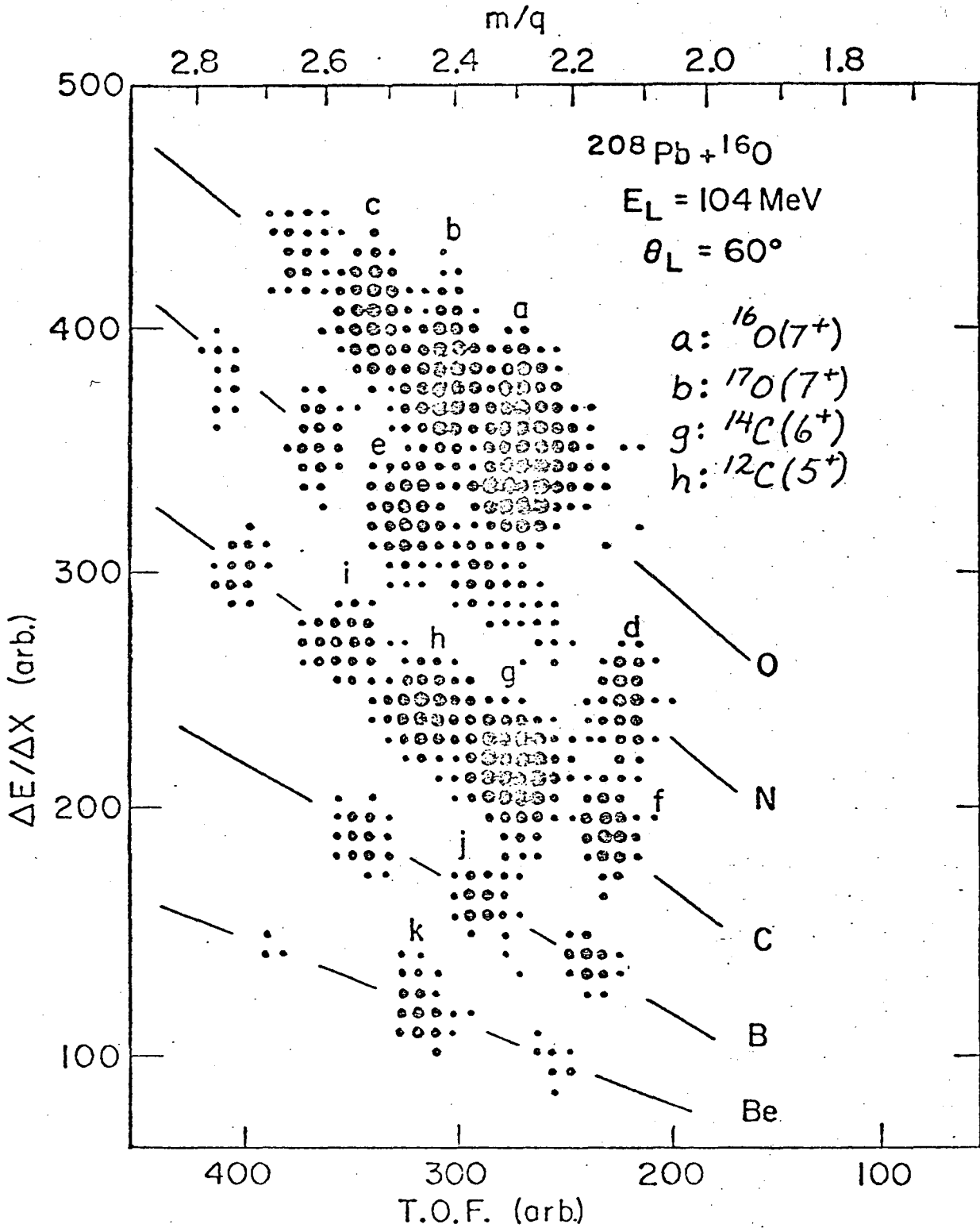
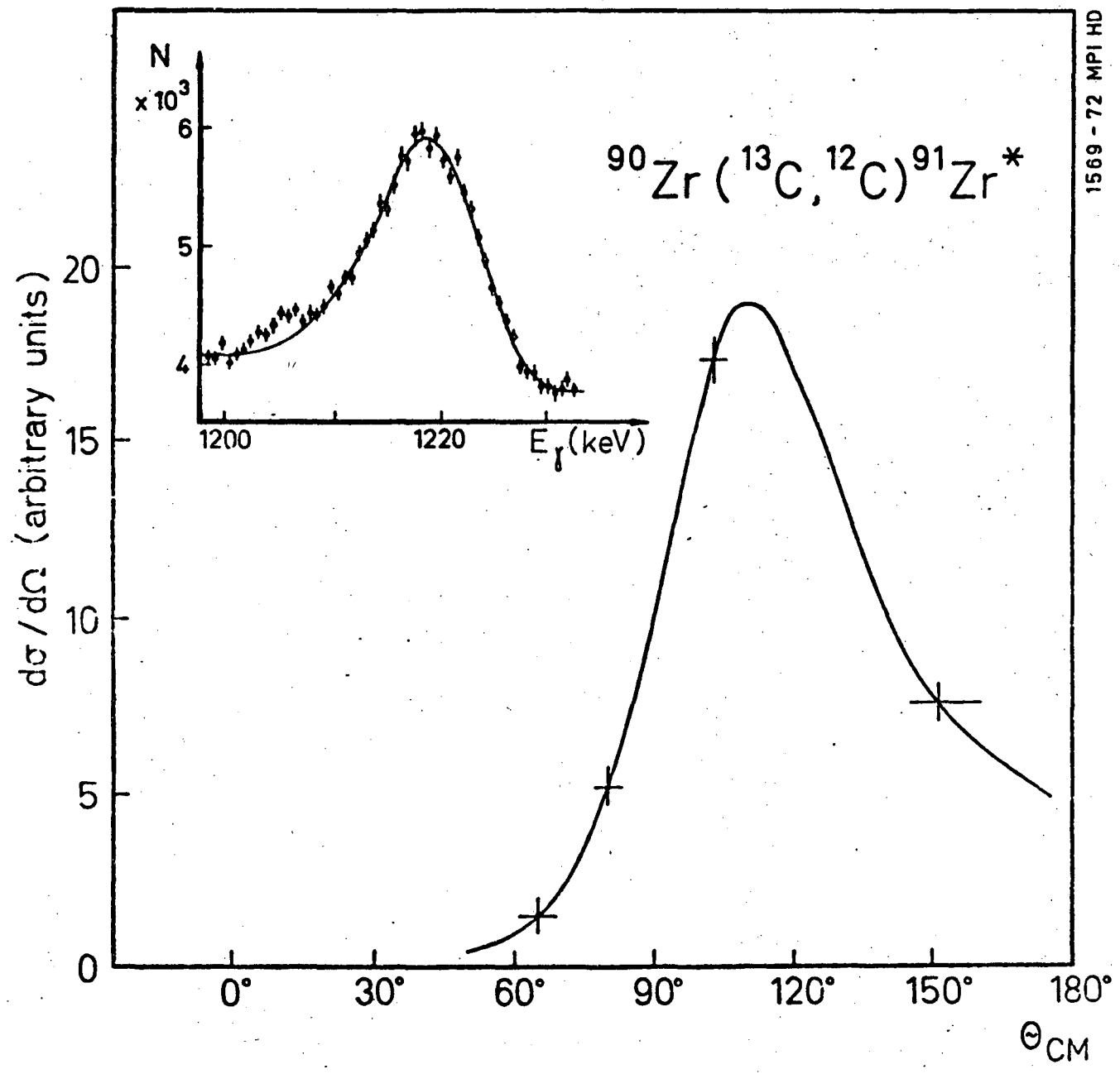


Fig. 1



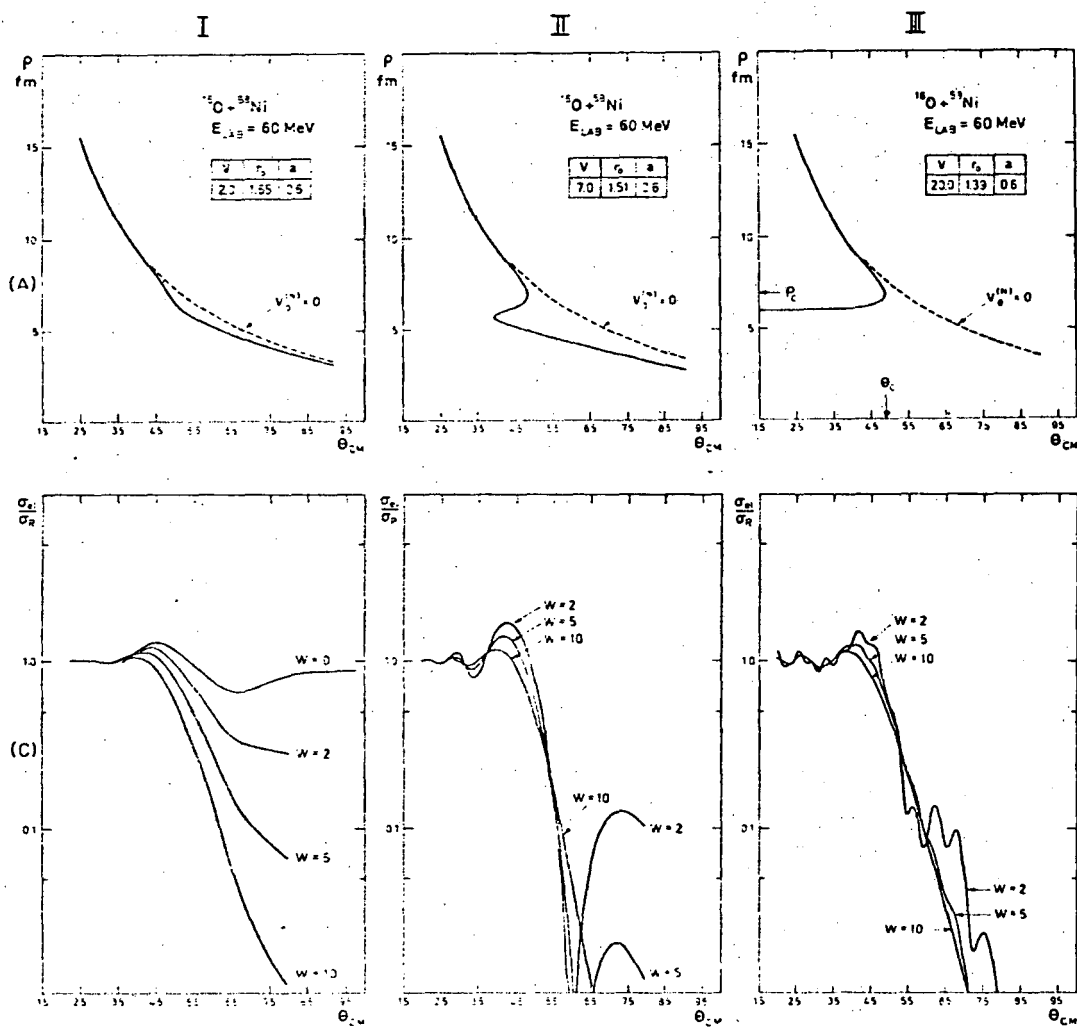
XBL 755-258

Fig. 2



1569 - 72 MPI HD

Fig. 3



XBL 733-265

Fig. 4

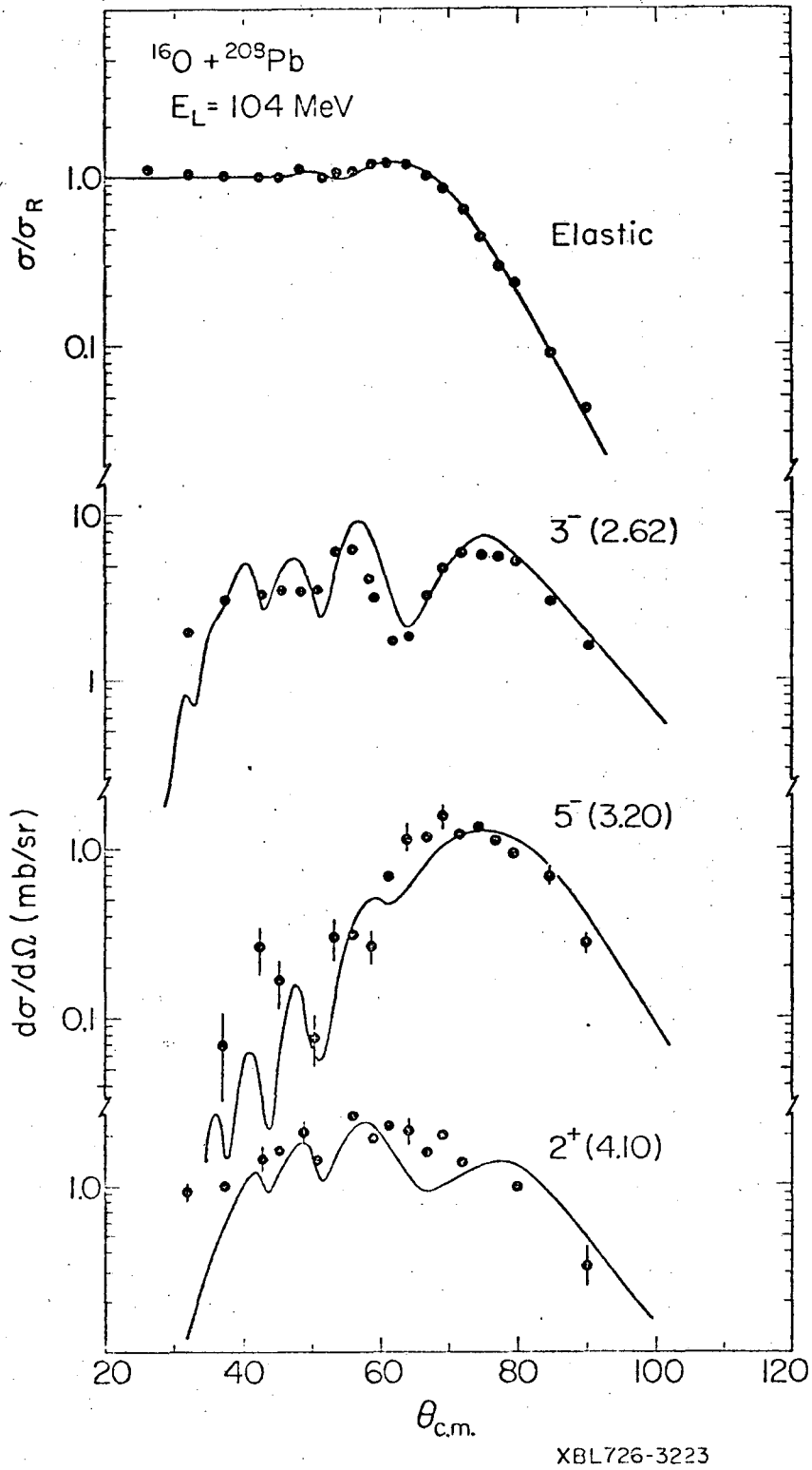
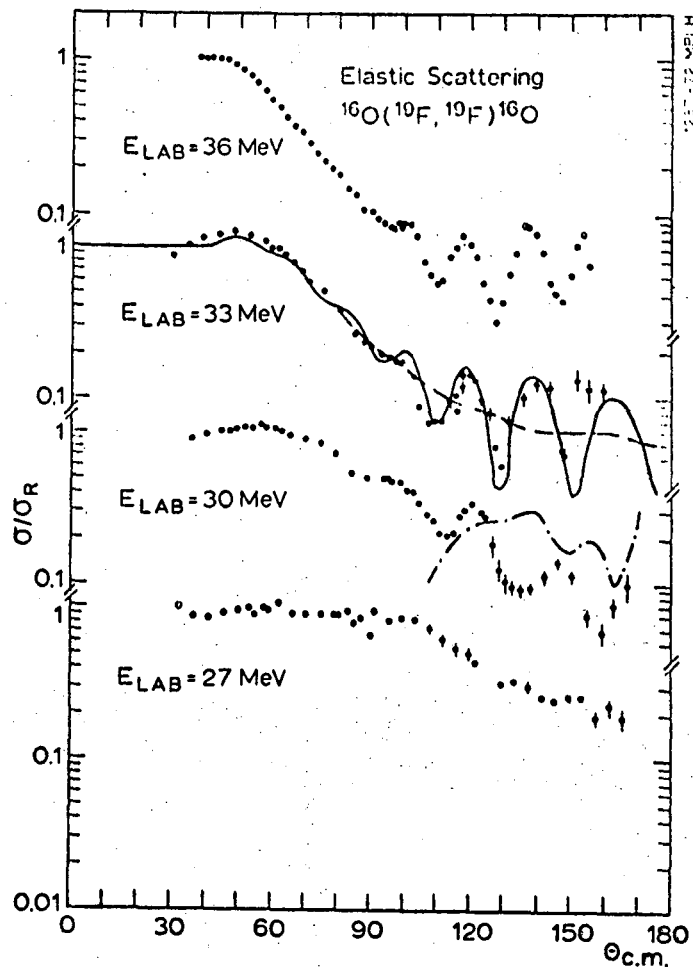
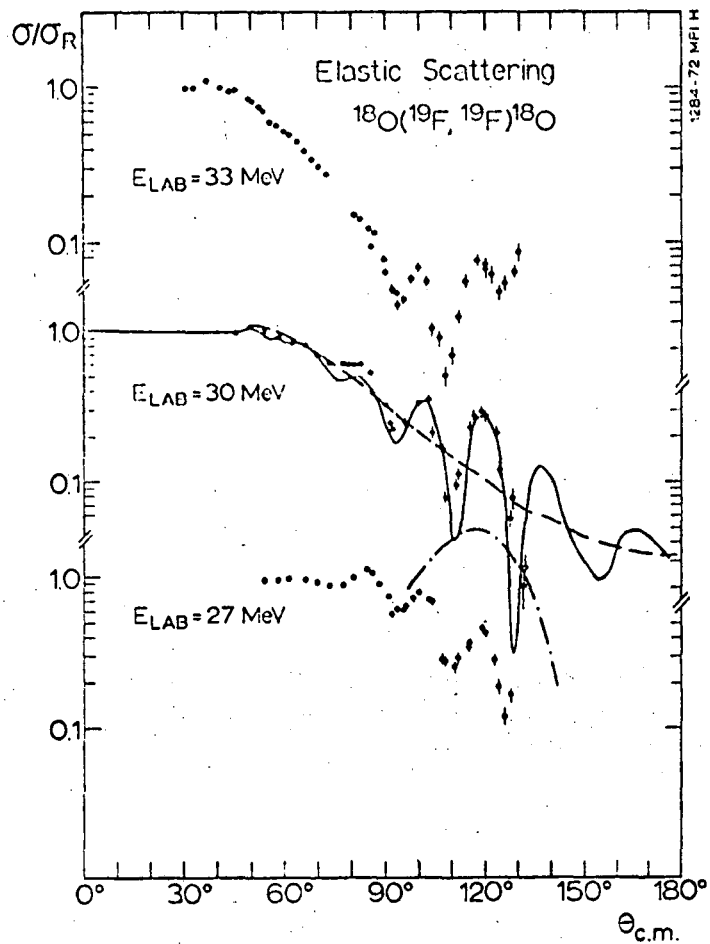


Fig. 5

FIG. 6



XBL 731-21

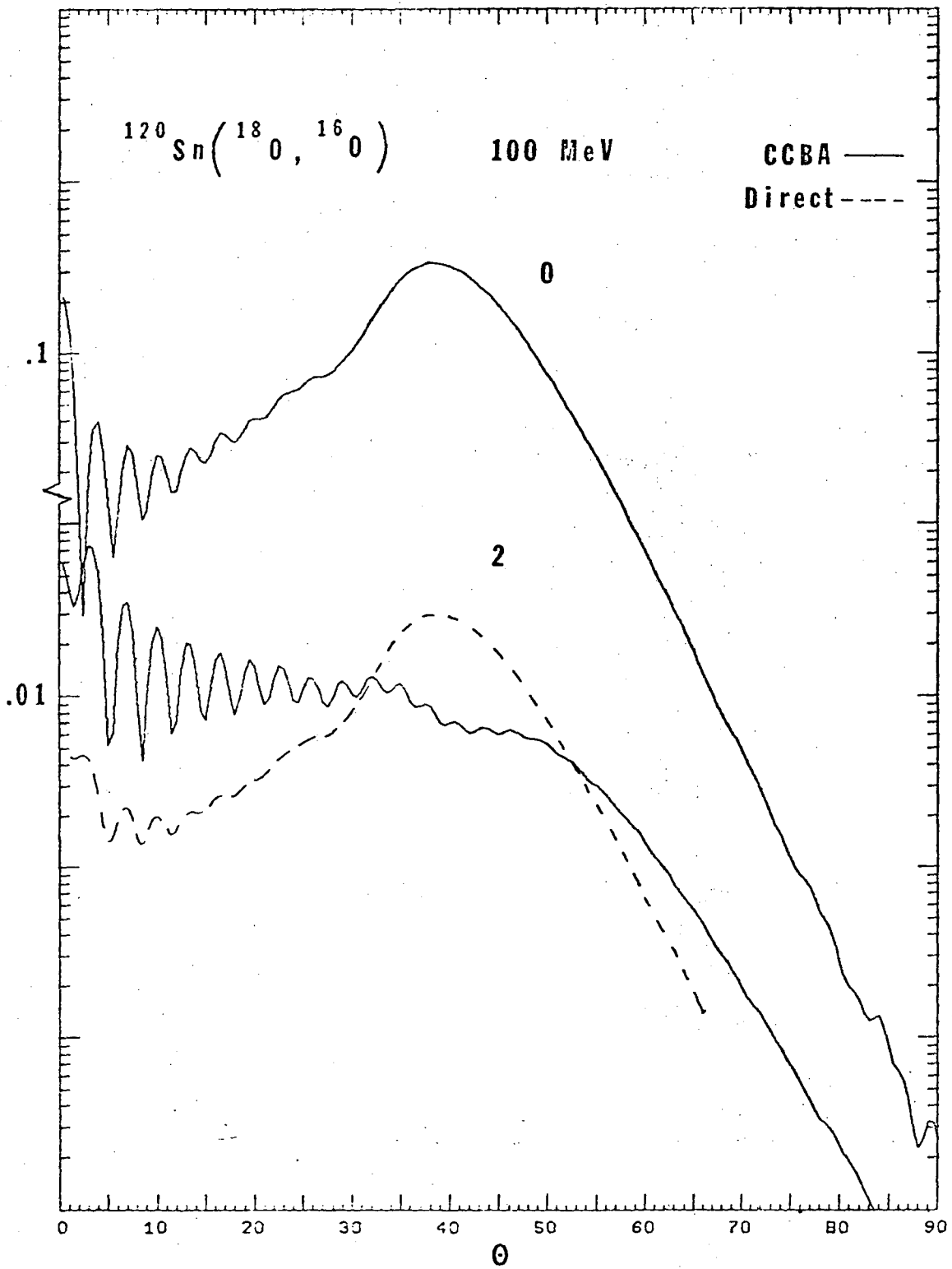


Fig. 7

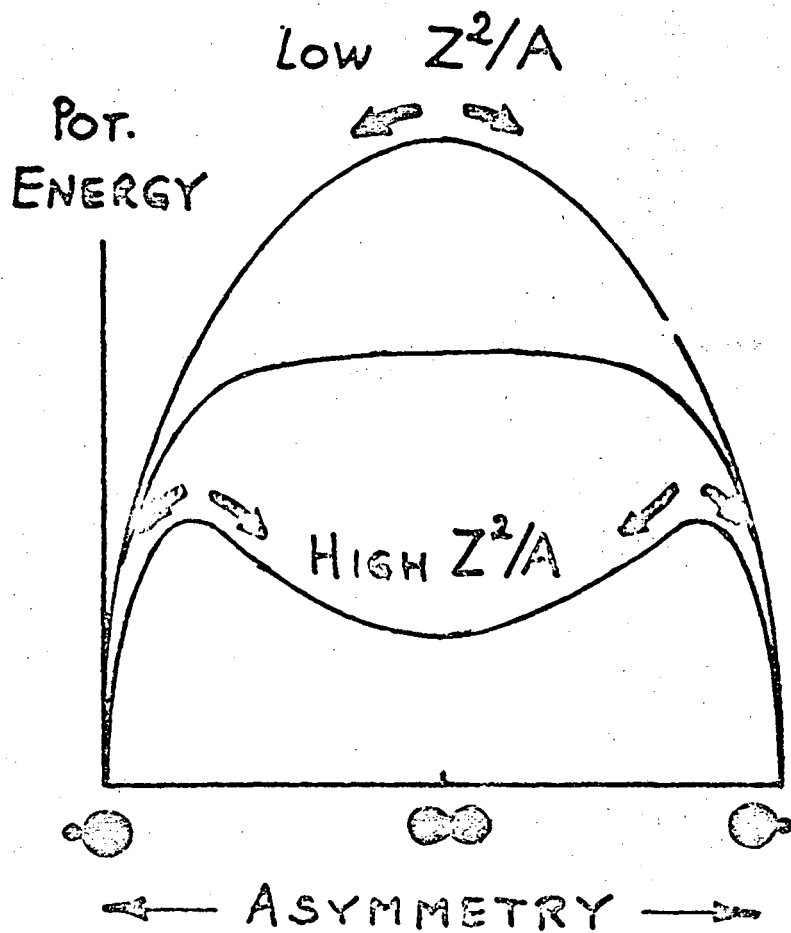
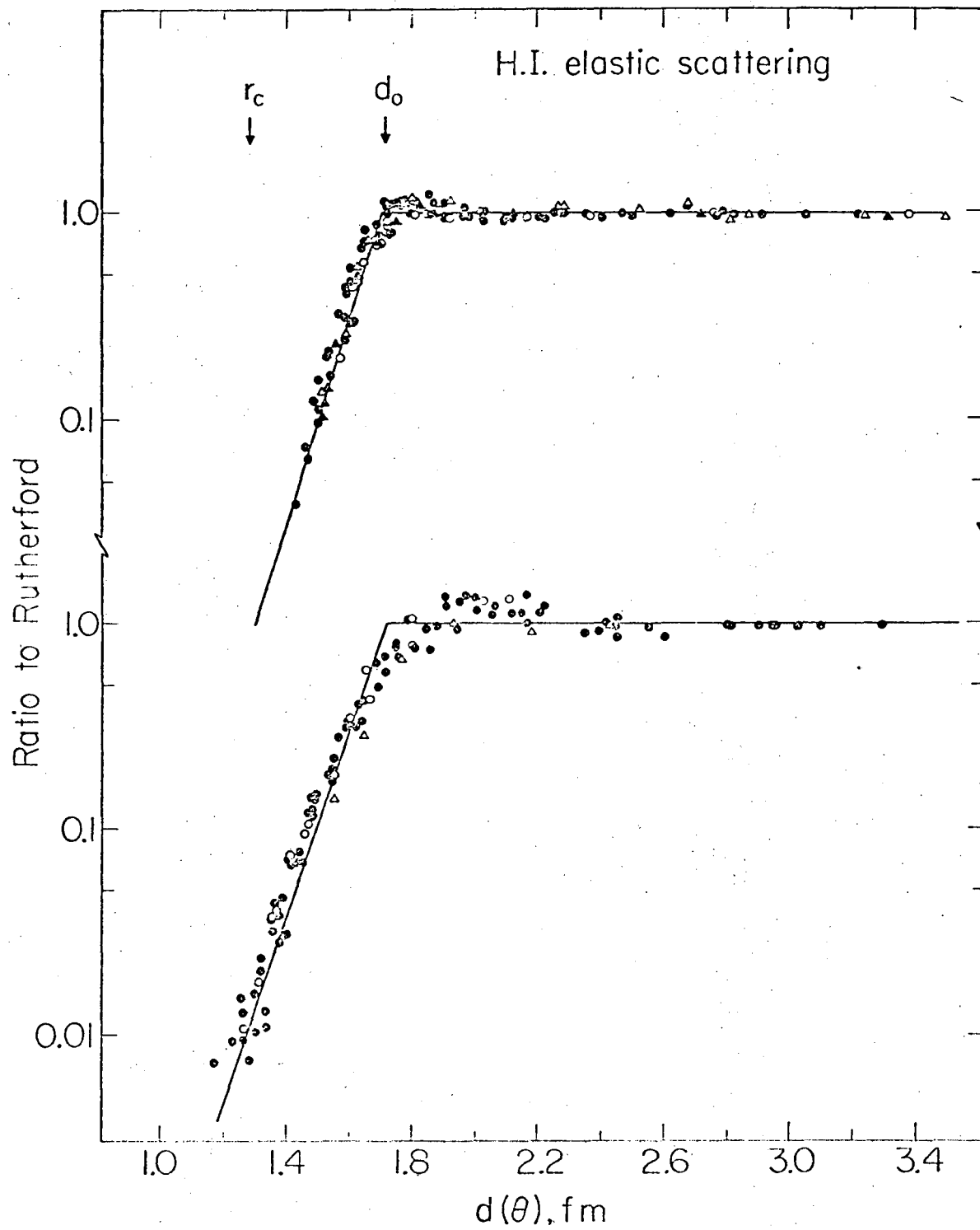
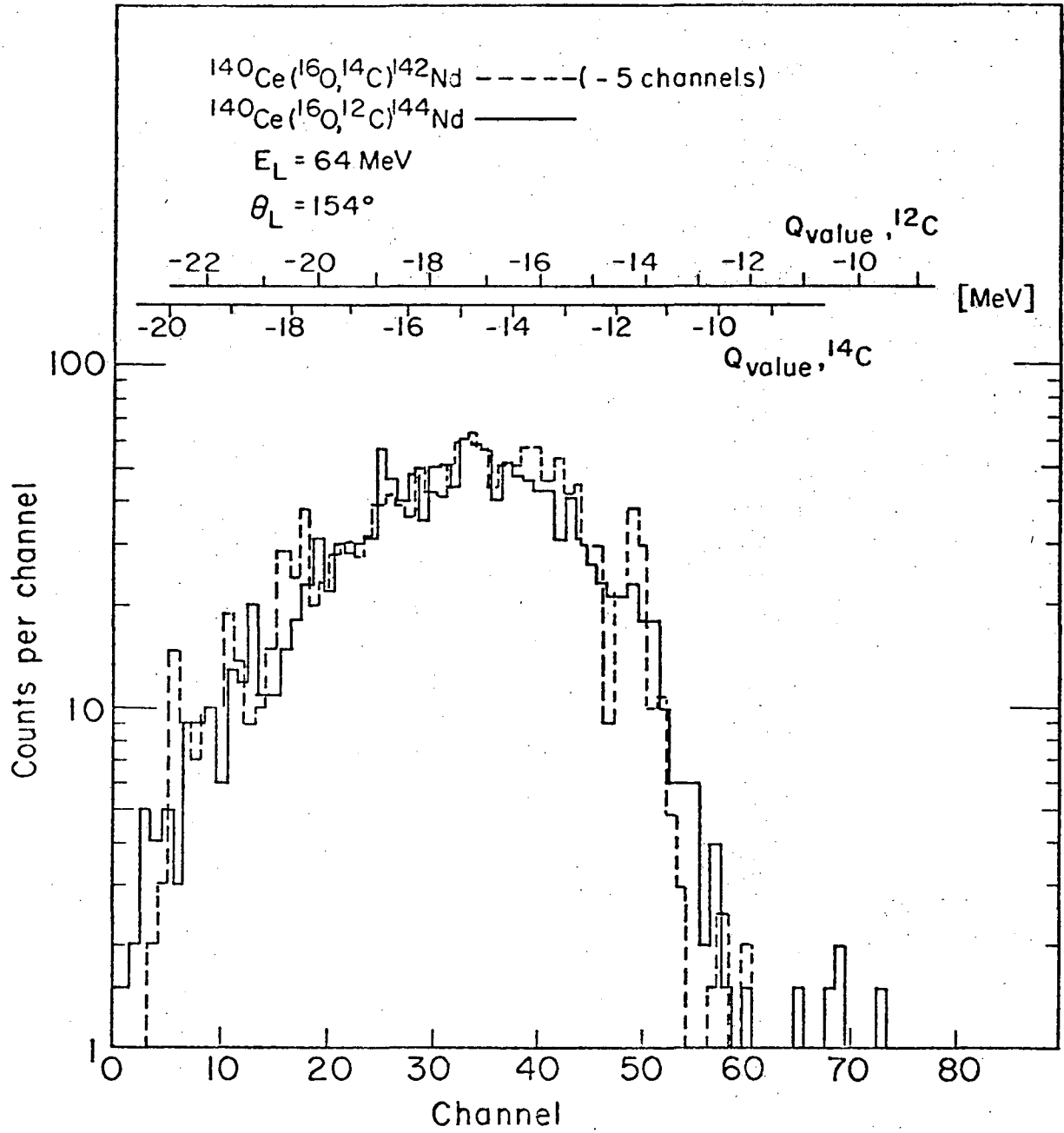


Fig. 8



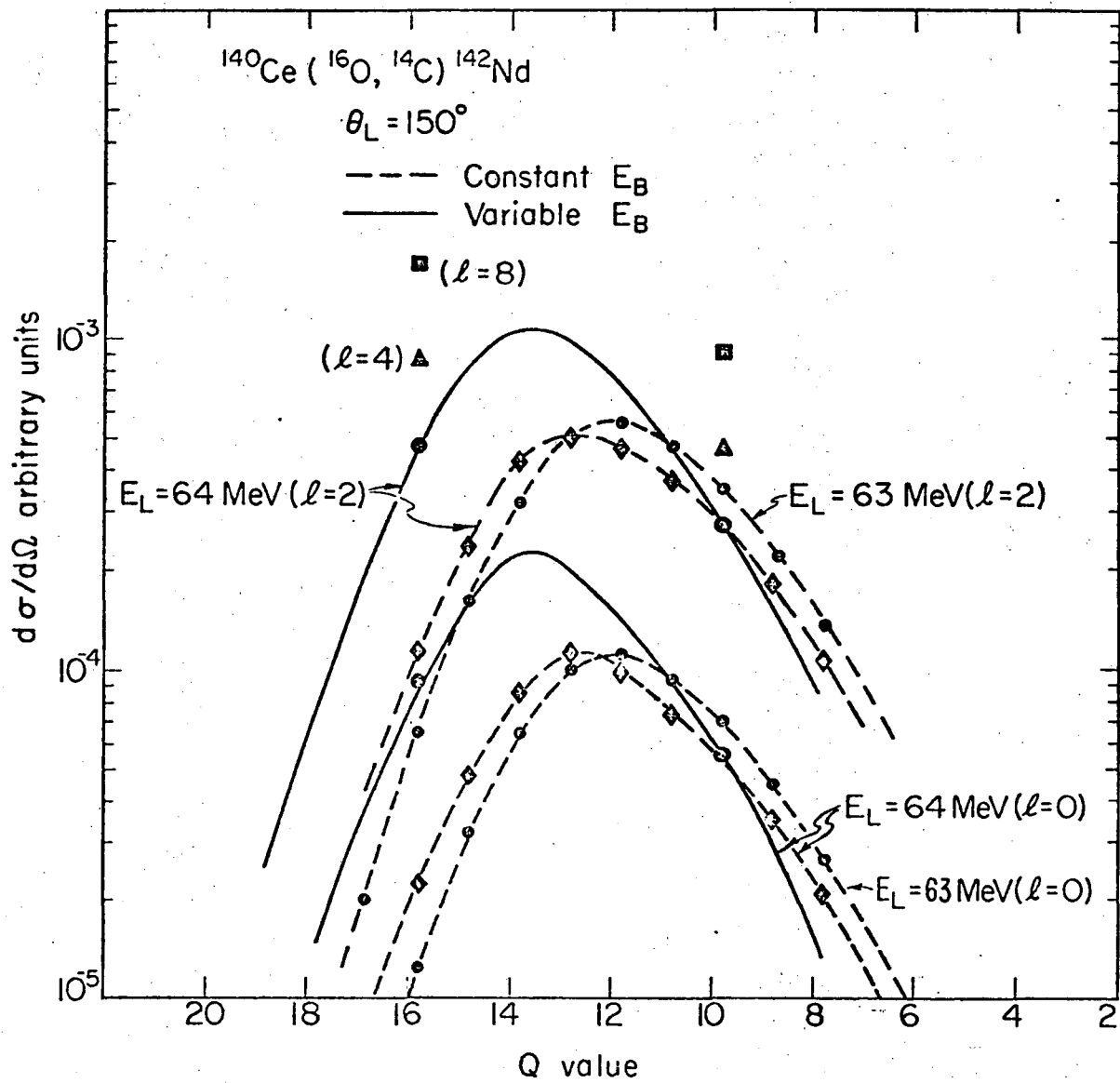
XBL723-2610

Fig. 9



XBL7211-4424

Fig. 10



XBL7211-4425

Fig. 11

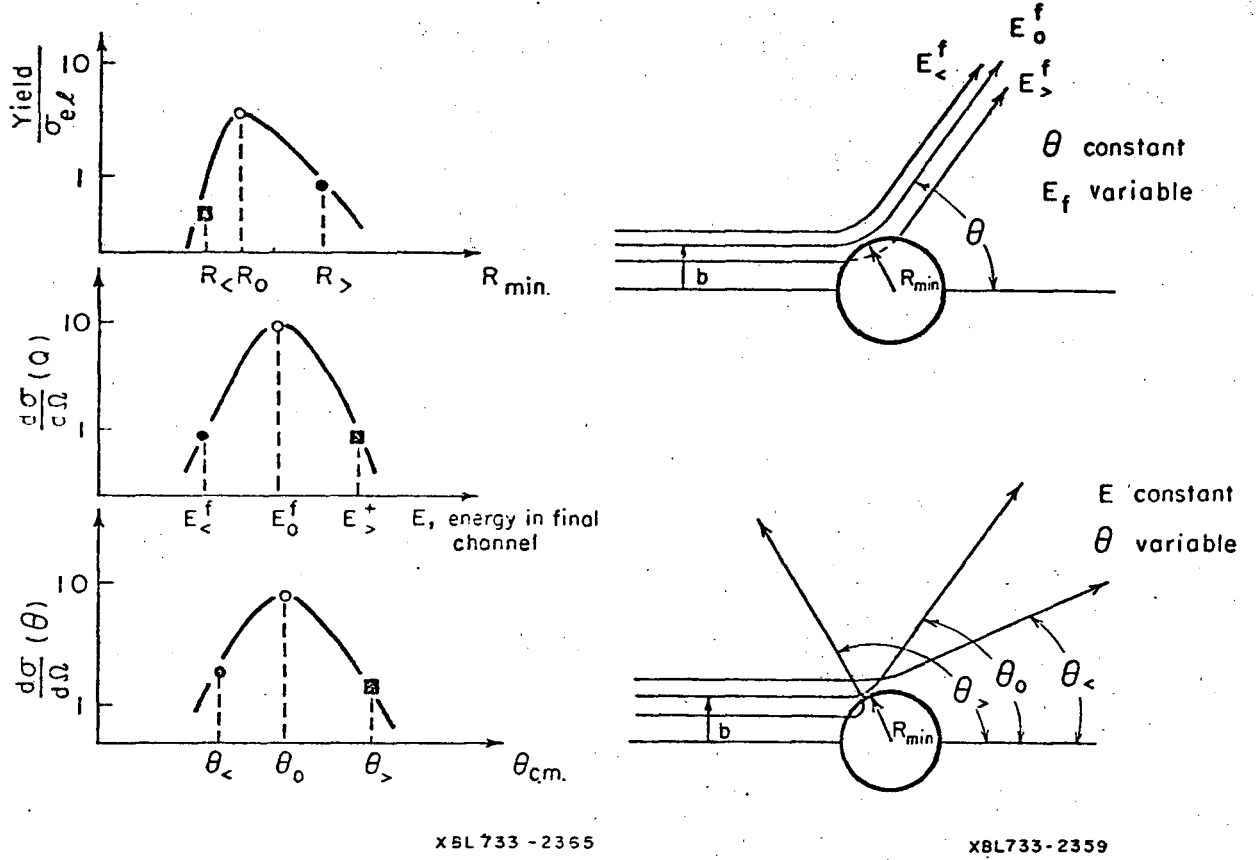


Fig. 12

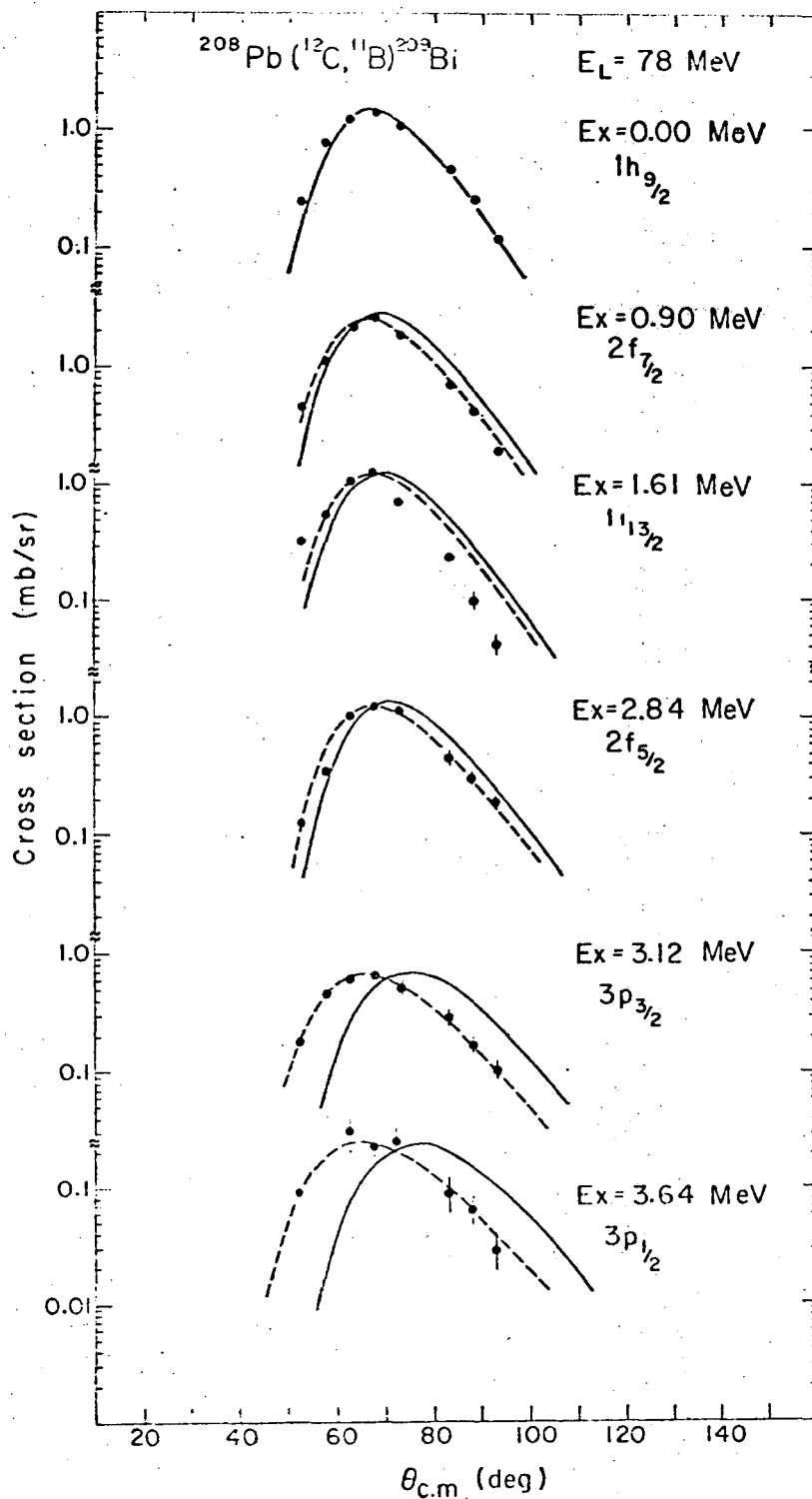
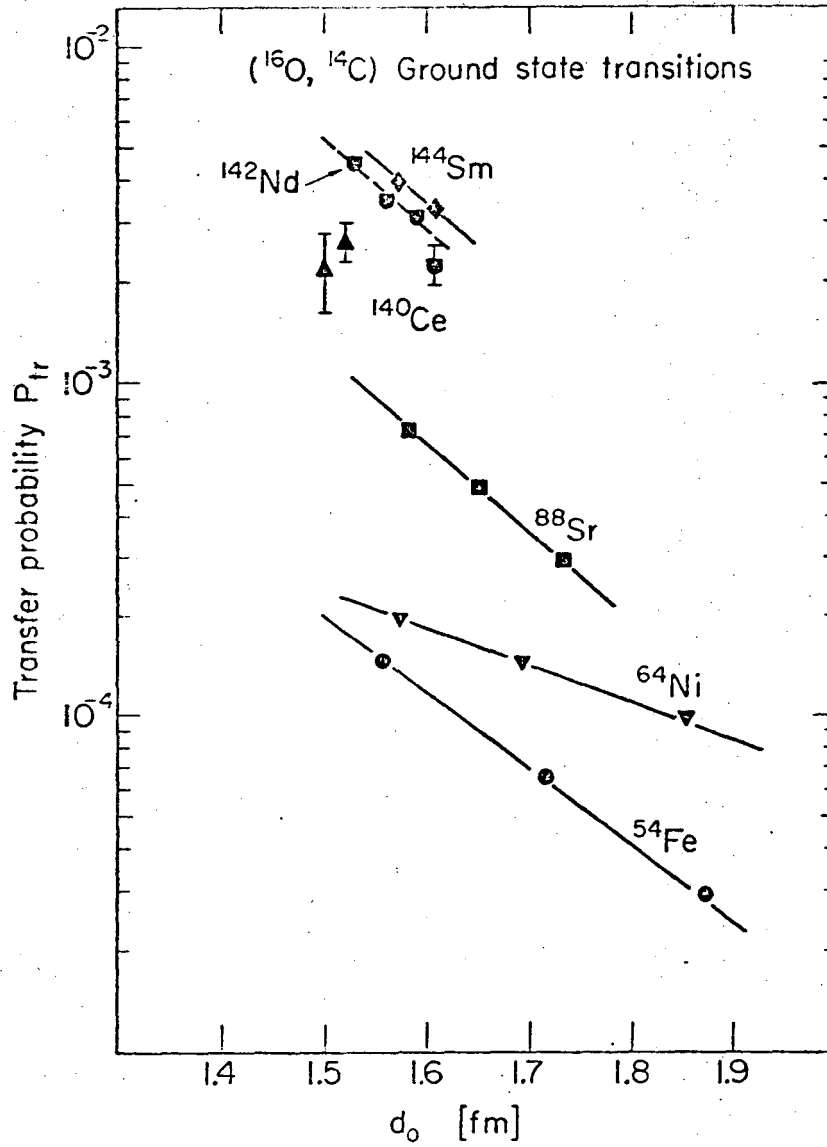
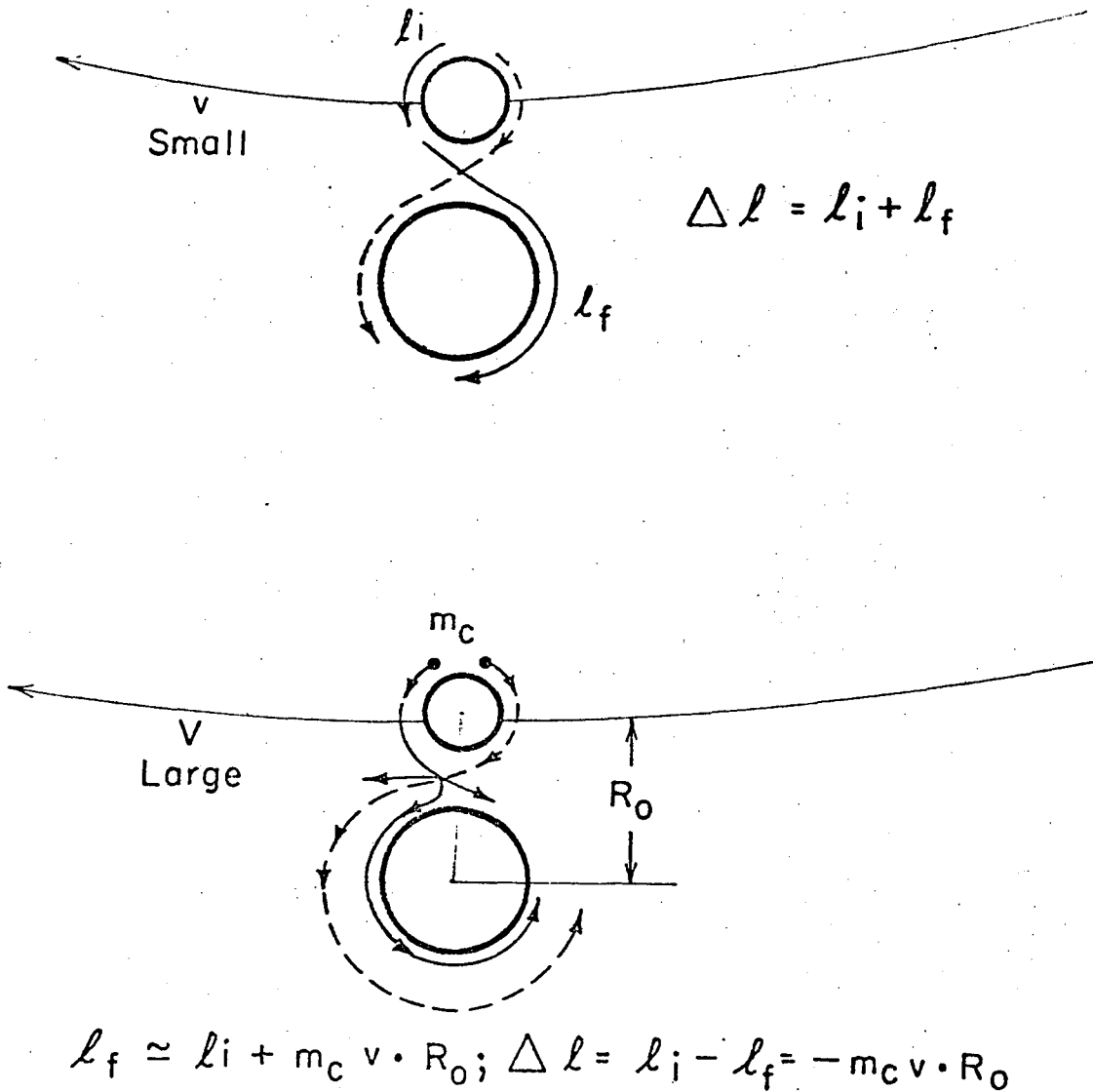


Fig. 13



XBL7212-4960

Fig. 14



XBL733-2358

Fig. 15

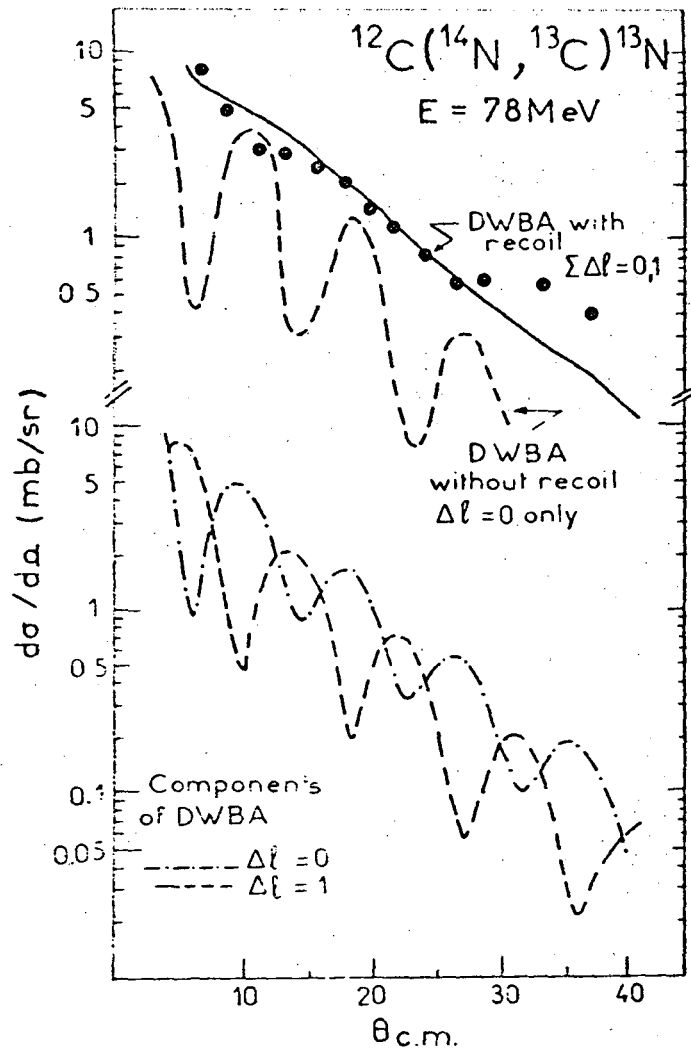
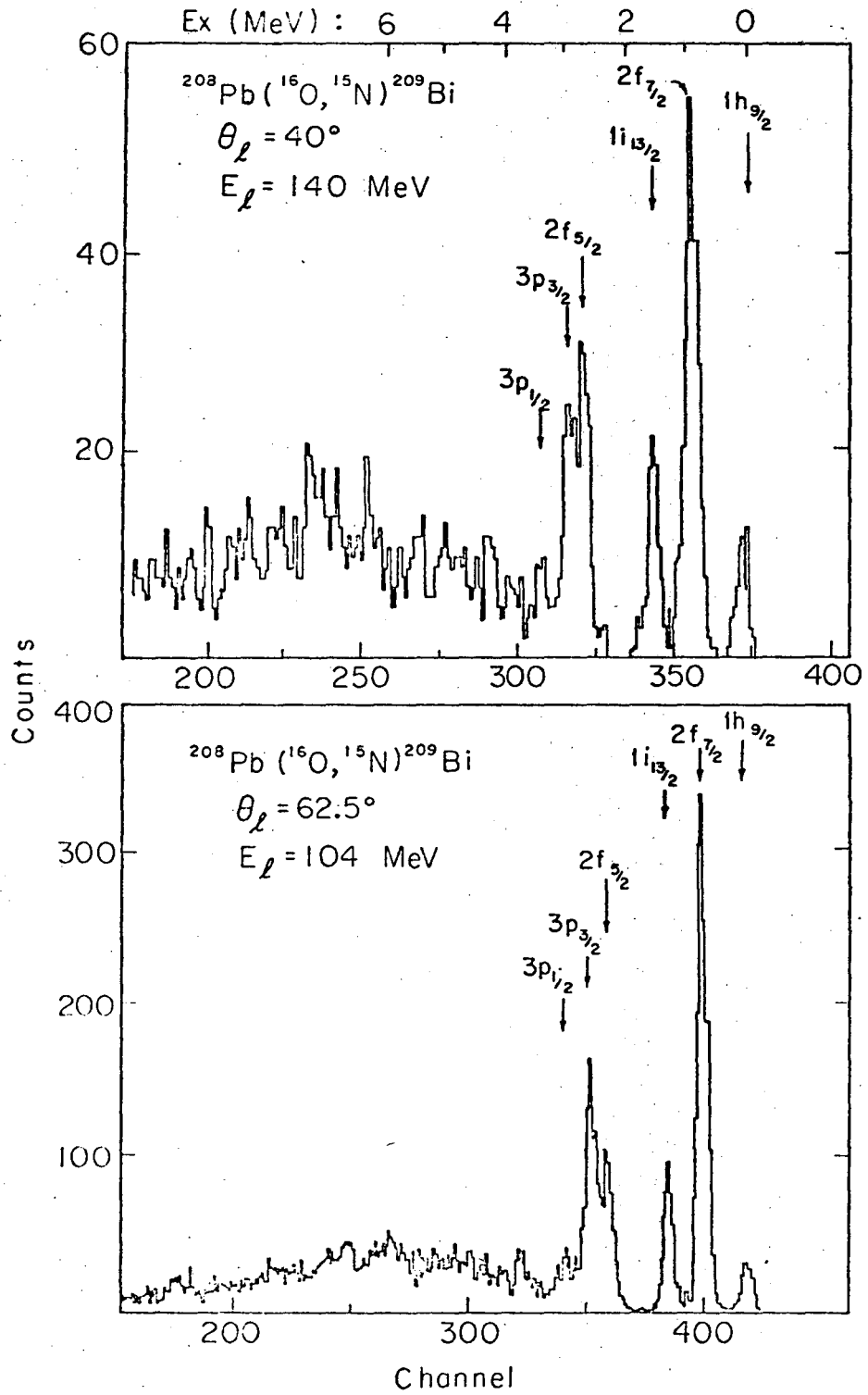


Fig. 16



XBL731-2145

Fig. 17

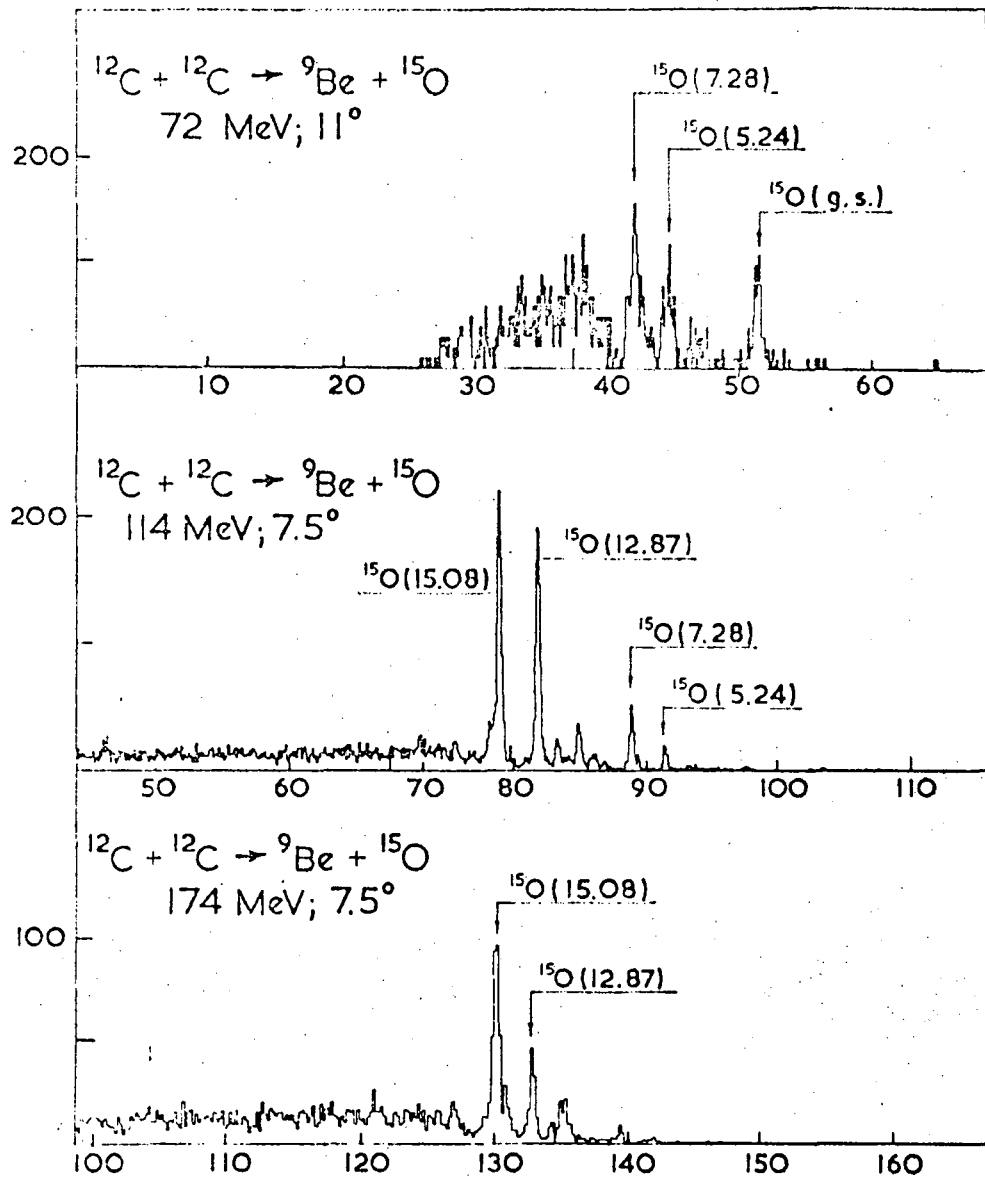
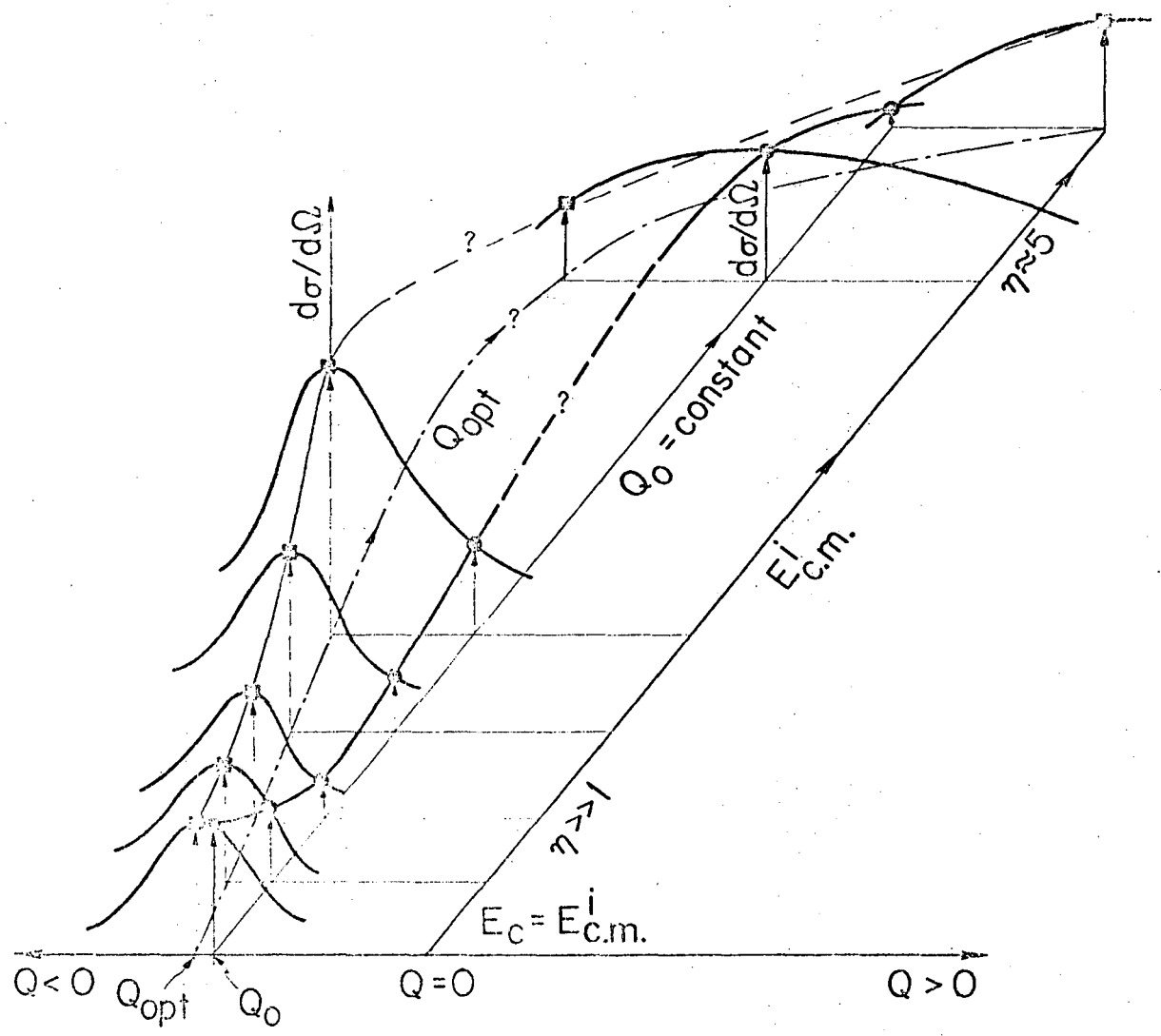
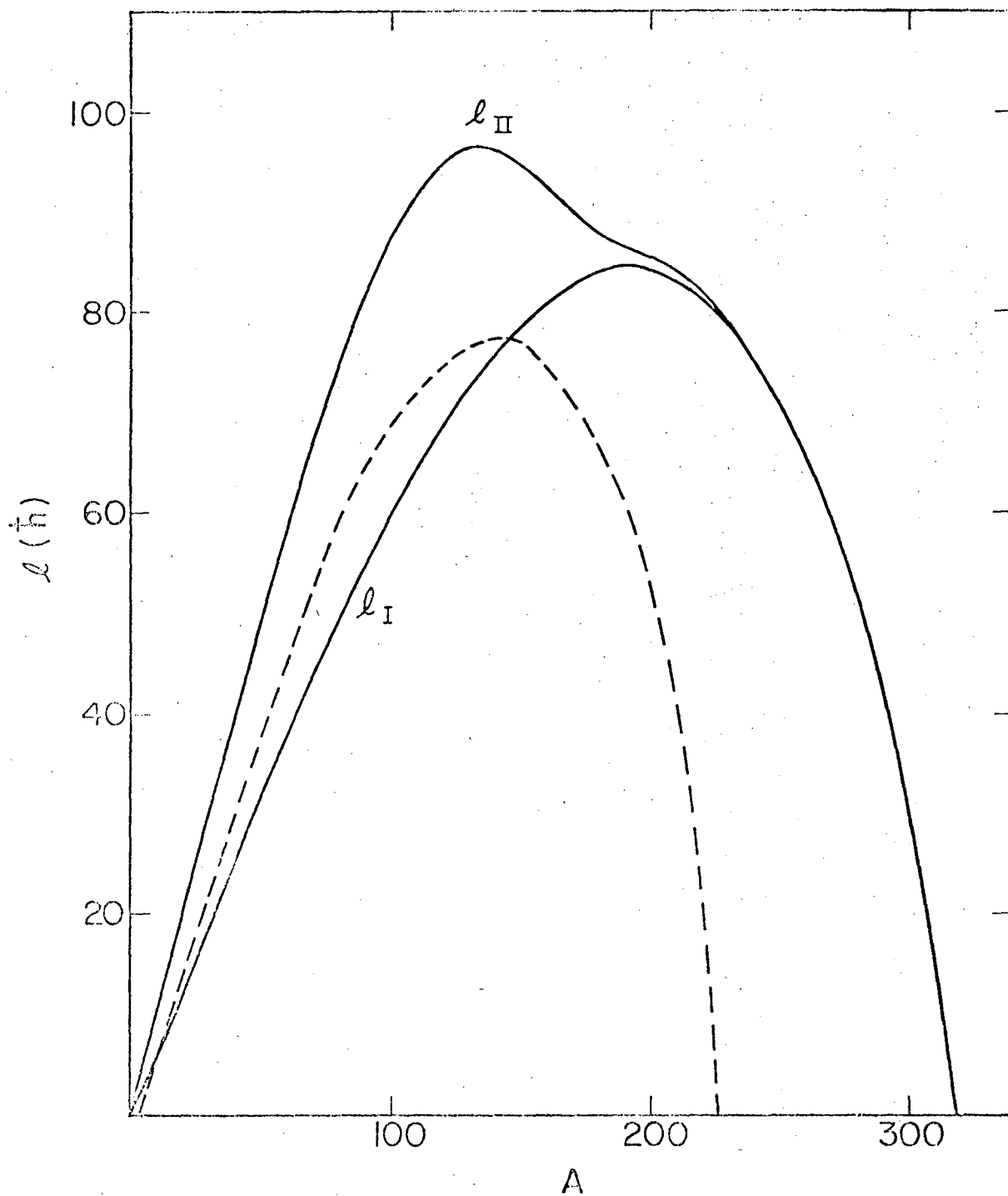


Fig. 18



XBL734-2742

Fig. 19



XBL7210-4342

Fig. 20

LEGAL NOTICE

This report was prepared as an account of work sponsored by the United States Government. Neither the United States nor the United States Atomic Energy Commission, nor any of their employees, nor any of their contractors, subcontractors, or their employees, makes any warranty, express or implied, or assumes any legal liability or responsibility for the accuracy, completeness or usefulness of any information, apparatus, product or process disclosed, or represents that its use would not infringe privately owned rights.

TECHNICAL INFORMATION DIVISION
LAWRENCE BERKELEY LABORATORY
UNIVERSITY OF CALIFORNIA
BERKELEY, CALIFORNIA 94720